17th International Conference on the Applications of Computer
Science and Mathematics in Architecture and Civil Engineering
K. Gürlebeck and C. Könke (eds.)
Weimar, Germany, 12–14 July 2006

HYBRID SOLID-LIQUID MODEL FOR GRANULAR MATERIAL

M. Göttlicher*

*Department of Civil Engineering, University of Applied Sciences,
Altonaer Str. 25, D-99085 Erfurt, Germany*
E-mail: goettlicher@fh-erfurt.de

Keywords: granular material, silo, single element system, steady-state flow.

Abstract. *Solid behavior as well as liquid behavior characterizes the flow of granular material in silos. The presented model is based on an appropriate interaction of a displacement field and a velocity field. The constitutive equations and the applied algorithm are developed from the exact solution for a standard case. The standard case evolves from a very tall vertical plane strain silo containing material that flows at a constant speed. Tension is not allowed at any point. The interaction between the flowing material and the walls is covered by a forced boundary condition resulting in an additional matrix for the solid component as well as for the liquid component. The resulting integral equations are designed to be solved directly.*

1 INTRODUCTION

Flows through chutes have been a topic of interest to many researchers for a long time. Theoretical and experimental studies of flows of cohesionless granular materials through chutes and channels have been conducted by Savage [7].

Pouliquen [5] discusses different flow configurations. A vertical chute flow is obtained when granular material flows in a silo made of two rough vertical planes in 2D or in a rough cylinder in 3D. In this case the force balance in the steady uniform regime predicts that the pressure is uniform across the silo but the shear stress varies linearly. Two finite shear bands are observed in experiments [4, 6]. In the interior of the silo a constant velocity distribution is observed in the quasi-static limit. Other steady-state flow configurations are plane shear, inclined plane and flow on a pile.

Das & Jenkins [2] consider steady, fully-developed flows of spheres under gravity in a vertical chute. Using balance equations, constitutive relations, and boundary conditions that result from kinetic theory, they calculate the fields of mean velocity, fluctuation velocity, and concentration across a chute for a variety of flow rates, particle parameters, and chute widths. They find two qualitatively different steady flow regimes. One is a dense flow regime with low mean velocity while the other is one with a dilute flow and higher mean velocity. As the volume flow rate increases the two solutions approach each other, and at some point, only one steady solution exists. Beyond this value of volume flow rate, not any steady solutions are observed. For a fixed volume flow rate, there is a critical chute width below which no steady flow is observed.

This paper proposes a hybrid solid-liquid model. The development of this new model starts from the vertical chute flow which is referred to as the standard case. It leads to a general formulation that describes the flow of granular material in silos.

2 STANDARD CASE

Considering a tall silo, a special situation evolves in that part of the structure that is far away from the surface and that is also far away from the bottom with its opening and its optional cone [4]. The material seams to be at rest, but at the same time it is flowing continuously. Neither a solid nor a liquid analysis describes this situation sufficiently.

In a very tall silo with a constant cross section, no changes of stresses and velocities take place in the vertical direction. Also no changes take place regarding time. The most important property of granular material is the fact that tensile stresses are not possible in the state of rest and in the state of flow. In the compression range, the material is assumed to behave perfectly elastic. Coulomb friction determines the interaction with the walls. The resulting situation is appropriate to focus on the analysis of the physical phenomenon.

The elastic analysis for the standard case with fixed boundary conditions on the walls results in a mere shearing deformation. Compression and tension have the same magnitude if no loads act on the top and bottom faces. A contradiction between the shear forces and the normal forces occurs on the walls regarding Coulomb friction.

A state of solid motion requires the presence of an appropriate constant vertical pressure. The resulting wall pressure leads to shear stresses according to Coulomb friction. They hold the equilibrium to the weight of the volume of the associated slice. The whole pile of material moves downwards as a solid. The gravitational energy is converted into heat energy at the walls.

Alternatively, the filling of the silo can be treated as a Newtonian fluid. To avoid tension in the interior, again a vertical pressure is postulated. Due to incompressibility, the required vertical pressure is smaller than in the elastic case. However, this pressure can have any value greater than the value that is required to avoid tension. The gravitational energy is converted into heat energy by friction in the interior of the Newtonian fluid.

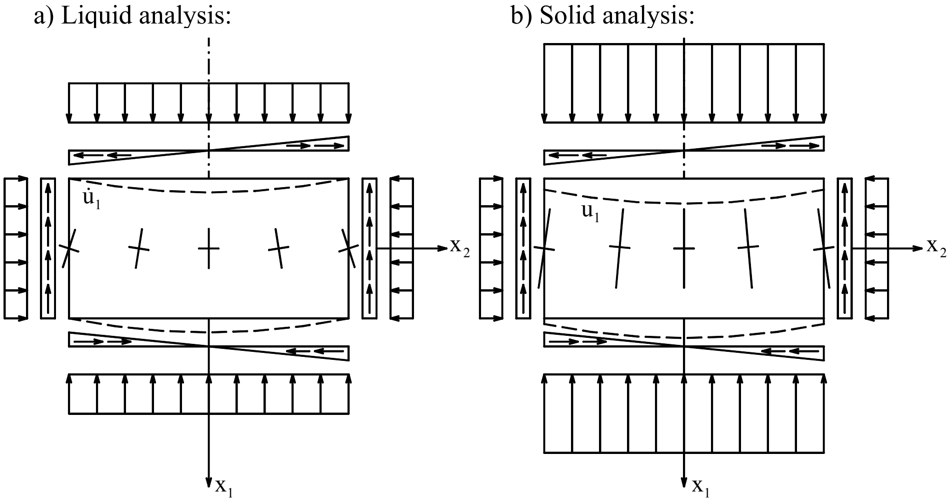

Fig. 1: Standard case: Surface loads and principal stresses

This paper proposes a hybrid description of the physical system. Elastic solid properties as well as viscous liquid properties characterize the flowing material. The discussion above shows that the vertical pressure required for the elastic solution is greater than the vertical pressure required for the viscous solution. For pressure levels between these limiting values, a hybrid elastic viscous behavior is postulated.

A fictive experiment supports this approach. A tall tube contains a pile of granular material. The tube starts to move upwards while the bottom remains at rest. For a constant speed of the tube, a steady state of motion in the interior of the filling evolves. The pressure on the bottom is expected to be lower than in the state of rest. For higher speeds of motion, the granular material behaves more and more like a liquid. The bottom pressure declines. If the speed of the tube exceeds a certain value, the continuity of the filling is lost.

These experimental aspects determine the development of an appropriate finite element model.

3 SOLID ANALYSIS

The derivation of the solid analysis is based on the principle of virtual displacements [1].

$$\int_V \boldsymbol{\sigma}^T \delta\boldsymbol{\varepsilon} dV - \int_V \mathbf{p}^T \delta\mathbf{u} dV - \int_A \mathbf{s}^T \delta\mathbf{u} dA = 0 \tag{1}$$

$\mathbf{u}$	displacements	$\mathbf{p}$	body load
$\boldsymbol{\sigma}$	stresses	V	volume
$\mathbf{s}$	surface load	A	surface

The strains are determined as derivatives of the displacements. For plane strain follows:

$$\boldsymbol{\varepsilon} = \begin{pmatrix} \varepsilon_{11} \\ \varepsilon_{22} \\ \varepsilon_{12} \end{pmatrix} = \mathbf{D}\mathbf{u} = \begin{pmatrix} \dfrac{\partial u_1}{\partial x_1} \\ \dfrac{\partial u_2}{\partial x_2} \\ \dfrac{\partial u_1}{\partial x_2} + \dfrac{\partial u_2}{\partial x_1} \end{pmatrix} \qquad \boldsymbol{\sigma} = \begin{pmatrix} \sigma_{11} \\ \sigma_{22} \\ \sigma_{12} \end{pmatrix} \tag{2}$$

The area A_S covers the cross section of the silo on the bottom and on the top of the considered part of the silo. The remaining area A_U covers the silo wall.

$$A_S + A_U = A \tag{3}$$

$$\int_A \mathbf{s}^T \delta\mathbf{u}\, dA = \int_{A_S} \mathbf{s}^T \delta\mathbf{u}\, dA + \int_{A_U} \mathbf{s}^T \delta\mathbf{u}\, dA \tag{4}$$

The silo wall is represented by a mixed boundary condition, since the displacement is restricted in the normal direction and the forces are restricted in tangential direction. Coulomb friction imposes a fixed relation between the horizontal und the vertical forces that act on the continuum.

$$\begin{aligned} s_t &= \mu \cdot s_n \\ u_n &= 0 \end{aligned} \qquad \mathbf{x} \in A_U \tag{5}$$

μ coefficient of wall friction

Displacements u_n normal to the wall are excluded. Tangential displacements u_t are possible.

$$\int_{A_U} \mathbf{s}^T \delta\mathbf{u}\, dA = \int_{A_U} \mu s_n \delta u_t\, dA \tag{6}$$

Tangential and normal components follow from the Cartesian components.

$$\mathbf{u}_A = \begin{pmatrix} u_n \\ u_t \end{pmatrix} = \mathbf{T} \cdot \mathbf{u} \qquad \mathbf{s}_A = \begin{pmatrix} s_n \\ s_t \end{pmatrix} = \mathbf{T} \cdot \mathbf{s} \tag{7}$$

$$\mathbf{s} = \begin{pmatrix} s_1 \\ s_2 \end{pmatrix} = \mathbf{M}^{\mathrm{T}} \boldsymbol{\sigma} \qquad \mathbf{x} \in \mathrm{A} \tag{8}$$

Transformation matrices:

$$\mathbf{T} = \begin{pmatrix} -n_1 & n_2 \\ n_2 & -n_1 \end{pmatrix} = \begin{pmatrix} \mathbf{t}_1^{\mathrm{T}} \\ \mathbf{t}_2^{\mathrm{T}} \end{pmatrix} \tag{9}$$

$$\mathbf{M}^{\mathrm{T}} = \begin{pmatrix} n_1 & 0 & n_2 \\ 0 & n_2 & n_1 \end{pmatrix} \qquad \mathbf{n} = \begin{pmatrix} n_1 \\ n_2 \end{pmatrix} \tag{10}$$

n vector normal to boundary

Eqs. (6) to (9) lead to

$$\int_{A_U} \mathbf{s}^{\mathrm{T}} \delta \mathbf{u} \, dA = \int_{A_U} \mu \, \mathbf{t}_1^{\mathrm{T}} \mathbf{M}^{\mathrm{T}} \boldsymbol{\sigma} \, \mathbf{t}_2^{\mathrm{T}} \delta \mathbf{u} \, dA \tag{11}$$

Elastic material properties are assumed. Instead of merely elastic behavior, more sophisticated and more accurate constitutive equations are appropriate.

$$\boldsymbol{\sigma} = \mathbf{E} \boldsymbol{\varepsilon} \tag{12}$$

The matrix of elasticity for plane strain is

$$\mathbf{E} = \frac{E(1-\nu)}{(1+\nu)(1-2\nu)} \begin{pmatrix} 1 & \dfrac{\nu}{(1-\nu)} & 0 \\ \dfrac{\nu}{(1-\nu)} & 1 & 0 \\ 0 & 0 & \dfrac{1-2\nu}{2(1-\nu)} \end{pmatrix} \tag{13}$$

E modulus of elasticity

ν Poisson’s ratio

Eqs. (11) and (12) are substituted in eq. (1).

$$\int_V \boldsymbol{\varepsilon}^{\mathrm{T}} \mathbf{E} \, \delta \boldsymbol{\varepsilon} \, dV - \int_V \mathbf{p}^{\mathrm{T}} \delta \mathbf{u} \, dV - \int_{A_S} \mathbf{s}^{\mathrm{T}} \delta \mathbf{u} \, dA + \int_{A_U} \mu \, \mathbf{t}_1^{\mathrm{T}} \mathbf{M}^{\mathrm{T}} \mathbf{E} \boldsymbol{\varepsilon} \, \mathbf{t}_2^{\mathrm{T}} \, \delta \mathbf{u} \, dA = 0 \tag{14}$$

The displacements in the interior and on the surface of the system are determined by functions of the nodal values.

$$\mathbf{u} = \mathbf{F}^{\mathrm{T}} \mathbf{w} \qquad \mathbf{x} \in V \qquad \mathbf{x} \in A_s \tag{15}$$

$$\boldsymbol{\varepsilon} = \mathbf{D} \mathbf{u} = \mathbf{D} \mathbf{F}^{\mathrm{T}} \mathbf{w} = \mathbf{B}^{\mathrm{T}} \mathbf{w} \tag{16}$$

$$\delta \mathbf{w}^{\mathrm{T}} \int_V \mathbf{B} \mathbf{E} \mathbf{B}^{\mathrm{T}} dV \mathbf{w} - \delta \mathbf{w}^{\mathrm{T}} \int_V \mathbf{F} \mathbf{p} \, dV - \delta \mathbf{w}^{\mathrm{T}} \int_{A_S} \mathbf{F} \mathbf{s} \, dA + \delta \mathbf{w}^{\mathrm{T}} \int_{A_U} \mathbf{F} \, \mathbf{t}_2 \mathbf{w}^{\mathrm{T}} \mathbf{B} \mathbf{E} \mathbf{M} \mu \, \mathbf{t}_1 \, dA = 0 \tag{17}$$

The last term is modified by transposition of the second scalar.

$$\mathbf{w}^{\mathrm{T}}\mathbf{B}\,\mathbf{E}\,\mathbf{M}\,\mu\,\mathbf{t}_1 = \mu\,\mathbf{t}_1^{\mathrm{T}}\mathbf{M}^{\mathrm{T}}\mathbf{E}\,\mathbf{B}^{\mathrm{T}}\mathbf{w} \tag{18}$$

$$\delta\mathbf{w}^{\mathrm{T}}\int_{V}\mathbf{B}\,\mathbf{E}\,\mathbf{B}^{\mathrm{T}}\mathrm{d}V\mathbf{w} - \delta\mathbf{w}^{\mathrm{T}}\int_{V}\mathbf{F}\,\mathbf{p}\,\mathrm{d}V - \delta\mathbf{w}^{\mathrm{T}}\int_{A_S}\mathbf{F}\,\mathbf{s}\,\mathrm{d}A + \delta\mathbf{w}^{\mathrm{T}}\int_{A_U}\mathbf{F}\,\mathbf{t}_2\,\mu\,\mathbf{t}_1^{\mathrm{T}}\mathbf{M}^{\mathrm{T}}\mathbf{E}\,\mathbf{B}^{\mathrm{T}}\mathrm{d}A\,\mathbf{w} = 0 \tag{19}$$

The wall forces result in a contribution to the stiffness matrix.

$$\delta\mathbf{w}^{\mathrm{T}}\left(\int_{V}\mathbf{B}\,\mathbf{E}\,\mathbf{B}^{\mathrm{T}}\mathrm{d}V + \int_{A_U}\mathbf{F}\,\mathbf{t}_2\,\mu\,\mathbf{t}_1^{\mathrm{T}}\,\mathbf{M}^{\mathrm{T}}\mathbf{E}\,\mathbf{B}^{\mathrm{T}}\mathrm{d}A\right)\mathbf{w} - \delta\mathbf{w}^{\mathrm{T}}\int_{V}\mathbf{F}\,\mathbf{p}\,\mathrm{d}V - \delta\mathbf{w}^{\mathrm{T}}\int_{A_S}\mathbf{F}\,\mathbf{s}\,\mathrm{d}A = 0 \tag{20}$$

For arbitrary variations follows

$$\left(\int_{V}\mathbf{B}\,\mathbf{E}\,\mathbf{B}^{\mathrm{T}}\mathrm{d}V + \int_{A_U}\mathbf{F}\,\mathbf{t}_2\,\mu\,\mathbf{t}_1^{\mathrm{T}}\mathbf{M}^{\mathrm{T}}\mathbf{E}\,\mathbf{B}^{\mathrm{T}}\mathrm{d}A\right)\mathbf{w} - \int_{V}\mathbf{F}\,\mathbf{p}\,\mathrm{d}V - \int_{A_S}\mathbf{F}\,\mathbf{s}\,\mathrm{d}A = 0 \tag{21}$$

The wall friction leads to an increased stiffness of the system. The behavior is similar to nodal boundaries that are directed with an angle according to the coefficient of wall friction. It is obvious that a meaningful solution exists always in this case. Those nodal boundaries however allow for lateral displacements that are excluded by the boundary conditions.

The solution of equation (21) is acceptable only if the wall pressure is negative (compression). Therefore, the proposed algorithm requires an a priori knowledge of the distribution of the surfaces A_U and A_S.

In the standard case the system has to be fixed in the vertical direction for numerical stability. No forces are allowed for these additional numerical boundaries. However a meaningful solution is possible only, if the normal wall pressure reaches the appropriate level. Otherwise irregular forces result for the numerical boundaries.

No problems will arise, if the bottom is fixed and if the free surface remains unloaded. This is the state of filling. The exact solution for the standard case arises, when the forces acting on the top surface and the displacements prescribed to the bottom face represent exactly the conditions of the standard case.

4 LIQUID ANALYSIS

The liquid model is formulated in an Eulerian framework [1, 9]. It is based on the principle of virtual velocities and has the same mathematical structure as the principle of virtual displacements. The derivation follows the previous chapter.

$$\int_{V}\boldsymbol{\sigma}^{\mathrm{T}}\delta\dot{\boldsymbol{\varepsilon}}\,\mathrm{d}V - \int_{V}\mathbf{p}^{\mathrm{T}}\delta\dot{\mathbf{u}}\,\mathrm{d}V - \int_{A}\mathbf{s}^{\mathrm{T}}\delta\dot{\mathbf{u}}\,\mathrm{d}A = 0 \tag{22}$$

$\dot{\mathbf{u}}$ velocities $\qquad$ $\dot{\boldsymbol{\varepsilon}}$ strain rates

$$\dot{\boldsymbol{\varepsilon}} = \begin{pmatrix} \dot{\varepsilon}_{11} \\ \dot{\varepsilon}_{22} \\ \dot{\varepsilon}_{12} \end{pmatrix} = \mathbf{D}\,\dot{\mathbf{u}} = \begin{pmatrix} \dfrac{\partial \dot{u}_1}{\partial x_1} \\ \dfrac{\partial \dot{u}_2}{\partial x_2} \\ \dfrac{\partial \dot{u}_1}{\partial x_2} + \dfrac{\partial \dot{u}_2}{\partial x_1} \end{pmatrix} \tag{23}$$

$$\begin{matrix} s_t = \mu \cdot s_n \\ \dot{u}_n = 0 \end{matrix} \qquad \mathbf{x} \in A_U \tag{24}$$

$$\int_{A_U} \mathbf{s}^T \delta \dot{\mathbf{u}} dA = \int_{A_U} \mu\, \mathbf{t}_1^T \mathbf{M}^T \boldsymbol{\sigma} \mathbf{t}_2^T \delta \dot{\mathbf{u}} dA \tag{25}$$

$$\int_V \boldsymbol{\sigma}^T \delta \dot{\boldsymbol{\varepsilon}} dV + \int_{A_U} \mu\, \mathbf{t}_1^T \mathbf{M}^T \boldsymbol{\sigma} \mathbf{t}_2^T \delta \dot{\mathbf{u}} dA - \int_V \mathbf{p}^T \delta \dot{\mathbf{u}} dV - \int_{A_S} \mathbf{s}^T \delta \dot{\mathbf{u}} dA = 0 \tag{26}$$

The velocities in the interior and on the surface of the system are determined by functions of the nodal values.

$$\dot{\mathbf{u}} = \mathbf{F}^T \dot{\mathbf{w}} \qquad \mathbf{x} \in V \qquad \mathbf{x} \in A_s \tag{27}$$

$$\dot{\boldsymbol{\varepsilon}} = \mathbf{D}\dot{\mathbf{u}} = \mathbf{D}\mathbf{F}^T \dot{\mathbf{w}} = \mathbf{B}^T \dot{\mathbf{w}} \tag{28}$$

$$\int_V \boldsymbol{\sigma}^T \mathbf{B}^T dV \delta \dot{\mathbf{w}} + \int_{A_U} \mu\, \mathbf{t}_1^T \mathbf{M}^T \boldsymbol{\sigma} \mathbf{t}_2^T \mathbf{F}^T dA \delta \dot{\mathbf{w}}$$

$$\int_V \boldsymbol{\sigma}^T \mathbf{B}^T dV \delta \dot{\mathbf{w}} + \int_{A_U} \mu\, \mathbf{t}_1^T \mathbf{M}^T \boldsymbol{\sigma} \mathbf{t}_2^T \mathbf{F}^T dA \delta \dot{\mathbf{w}} - \int_V \mathbf{p}^T \mathbf{F}^T dV \delta \dot{\mathbf{w}} - \int_{A_S} \mathbf{s}^T \mathbf{F}^T dA \delta \dot{\mathbf{w}} = 0 \tag{29}$$

$$\int_V \mathbf{B}\boldsymbol{\sigma} dV + \int_{A_U} \mathbf{F}\mathbf{t}_2 \mu\, \mathbf{t}_1^T \mathbf{M}^T \boldsymbol{\sigma} dA - \int_V \mathbf{F}\mathbf{p} dV - \int_{A_S} \mathbf{F}\mathbf{s} dA = 0 \tag{30}$$

The stresses $\boldsymbol{\sigma}$ depend on the strain rate $\dot{\boldsymbol{\varepsilon}}$ and the pressure a.

$$\boldsymbol{\sigma} = \mathbf{C}\dot{\boldsymbol{\varepsilon}} + \boldsymbol{\sigma}_p \tag{31}$$

$$\mathbf{C} = \begin{pmatrix} 2 & & \\ & 2 & \\ & & 1 \end{pmatrix} \eta \qquad \boldsymbol{\sigma}_p = \begin{pmatrix} a \\ a \\ 0 \end{pmatrix} \tag{32}$$

C matrix of viscosity
η viscosity
a pressure

The pressure interpolation is based on the following approximation:

$$a = \mathbf{g}^T \mathbf{a} \tag{33}$$

$$\boldsymbol{\sigma}_p = \mathbf{G}^T \mathbf{a} \tag{34}$$

$$\boldsymbol{\sigma} = \mathbf{C}\,\mathbf{B}^T \dot{\mathbf{w}} + \mathbf{G}^T \mathbf{a} \tag{35}$$

The treatment of viscous flow can be compared with the treatment of an incompressible elastic solid [8]. The velocities of the liquid then are related to the displacements of the solid.

$$\left(\int_V \mathbf{B}\,\mathbf{C}\,\mathbf{B}^T dV + \int_{A_U} \mathbf{F}\,\mathbf{t}_2 \mu \mathbf{t}_1^T \mathbf{M}^T \mathbf{C}\,\mathbf{B}^T dA \right) \dot{\mathbf{w}} + \ldots$$

$$\ldots + \left(\int_V \mathbf{B}\,\mathbf{G}^T dV + \int_{A_U} \mathbf{F}\,\mathbf{t}_2 \mu \mathbf{t}_1^T \mathbf{M}^T \mathbf{G}^T dA \right) \mathbf{a} - \int_V \mathbf{F}\,\mathbf{p}\, dV - \int_{A_S} \mathbf{F}\,\mathbf{s}\, dA = 0 \tag{36}$$

In addition, the fulfillment of the continuity condition is required.

$$\varepsilon_v = \frac{\partial \dot{u}_1}{\partial x_1} + \frac{\partial \dot{u}_2}{\partial x_2} = 0$$

$$\mathbf{d}\dot{\mathbf{u}} = \mathbf{d}\mathbf{F}^T \dot{\mathbf{w}} = \mathbf{H}^T \dot{\mathbf{w}} = 0 \tag{37}$$

A virtual pressure acts on the volumetric strain rates. The integral is zero.

$$\int_V \mathbf{d}\dot{\mathbf{u}} \delta \mathbf{a}\, dV = \delta \mathbf{a}^T \int_V \mathbf{g}\,\mathbf{H}^T dV \dot{\mathbf{w}} = 0 \tag{38}$$

For arbitrary variation follows:

$$\int_V \mathbf{g}\,\mathbf{H}^T dV \dot{\mathbf{w}} = 0 \tag{39}$$

A lower order of interpolation of the pressure a compared with that of the velocities $\dot{\mathbf{u}}$ is desirable only to avoid over-constraints [9].

No tension is permitted in the interior of the solution area. Sliding between liquid and wall is possible.

5 ELASTIC VISCOUS MODEL

The material is considered to consist of an elastic component and an incompressible viscous component. The distribution between both components depends on the material properties especially on the relation of the shear modulus and the dynamic viscosity. The velocities for the liquid part and the displacements for the elastic part are represented by the same variables.

$$\int \boldsymbol{\sigma}^T \delta \dot{\boldsymbol{\varepsilon}}\, dV - \int \mathbf{p}^T \delta \dot{\mathbf{u}}\, dV - \int \mathbf{s}^T \delta \dot{\mathbf{u}}\, dA = 0 \tag{40}$$

The derivation follows the solid and liquid analysis.

$$\left(\int_V \mathbf{B}(\mathbf{E}+\mathbf{C})\mathbf{B}^T dV + \int_{A_U} \mathbf{F}\,\mathbf{t}_2 \mu\, \mathbf{t}_1^T \mathbf{M}^T (\mathbf{E}+\mathbf{C})\mathbf{B}^T dA \right) \dot{\mathbf{w}} - \int_V \mathbf{F}\,\mathbf{p}\, dV - \int_{A_S} \mathbf{F}\,\mathbf{s}\, dA = 0 \qquad (41)$$

This approach already refers to the hybrid nature of granular flow. The following chapter presents a more flexible formulation that also includes the continuity condition.

6 HYBRID SOLID-LIQUID MODEL

The hybrid solid-liquid model postulates two independent sets of variables. A displacement field and a velocity field cover the solution area. The mere solid solution and the mere liquid solution are unique.

The external loads **p** and **s** consist of two parts. $\mathbf{p}_S$ and $\mathbf{s}_S$ act on the solid part, $\mathbf{p}_L$ and $\mathbf{s}_L$ act on the liquid part of the hybrid system.

$$\mathbf{p} = \mathbf{p}_S + \mathbf{p}_L \qquad (42)$$

$$\mathbf{s} = \mathbf{s}_S + \mathbf{s}_L \qquad (43)$$

$$\left(\int_V \mathbf{B}\mathbf{E}\mathbf{B}^T dV + \int_{A_U} \mathbf{F}\,\mathbf{t}_2 \mu\, \mathbf{t}_1^T \mathbf{M}^T \mathbf{E}\mathbf{B}^T dA \right) \mathbf{w} - \int_V \mathbf{F}\,\mathbf{p}_S\, dV - \int_{A_S} \mathbf{F}\,\mathbf{s}_S\, dA = 0 \qquad (44)$$

$$\left(\int_V \mathbf{B}\mathbf{C}\mathbf{B}^T dV + \int_{A_U} \mathbf{F}\,\mathbf{t}_2 \mu\, \mathbf{t}_1^T \mathbf{M}^T \mathbf{C}\mathbf{B}^T dA \right) \dot{\mathbf{w}} + \ldots$$

$$\ldots + \left(\int_V \mathbf{B}\mathbf{G}^T dV + \int_{A_U} \mathbf{F}\,\mathbf{t}_2 \mu\, \mathbf{t}_1^T \mathbf{M}^T \mathbf{G}^T dA \right) \mathbf{a} - \int_V \mathbf{F}\,\mathbf{p}_L\, dV - \int_{A_S} \mathbf{F}\,\mathbf{s}_L\, dA = 0 \qquad (45)$$

$$\int_V \mathbf{g}\,\mathbf{H}^T dV \dot{\mathbf{w}} = 0 \qquad (46)$$

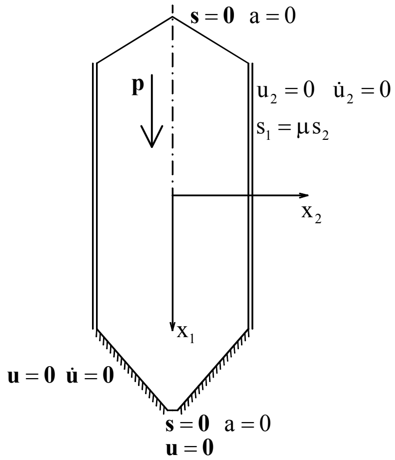

Fig. 2. Silo: Boundary conditions

These equations cannot be solved directly, since the distribution of the total load on both components is not unique.

Eqs. (44) and (45) require the minimum of potential energy for both, the solid part and the liquid part separately. Both parts together have to provide the overall equilibrium as indicated in the eqs. (42) and (43). Eqs. (44) and (45) are added.

$$\left(\int_V \mathbf{B}\mathbf{E}\mathbf{B}^{\mathrm{T}}\mathrm{d}V + \int_{A_U} \mathbf{F}\mathbf{t}_2\mu\mathbf{t}_1^{\mathrm{T}}\mathbf{M}^{\mathrm{T}}\mathbf{E}\mathbf{B}^{\mathrm{T}}\mathrm{d}A\right)\mathbf{w} + \left(\int_V \mathbf{B}\mathbf{C}\mathbf{B}^{\mathrm{T}}\mathrm{d}V + \int_{A_U} \mathbf{F}\mathbf{t}_2\mu\mathbf{t}_1^{\mathrm{T}}\mathbf{M}^{\mathrm{T}}\mathbf{C}\mathbf{B}^{\mathrm{T}}\mathrm{d}A\right)\dot{\mathbf{w}} + \ldots$$

$$\ldots + \left(\int_V \mathbf{B}\mathbf{G}^{\mathrm{T}}\mathrm{d}V + \int_{A_U} \mathbf{F}\mathbf{t}_2\mu\mathbf{t}_1^{\mathrm{T}}\mathbf{M}^{\mathrm{T}}\mathbf{G}^{\mathrm{T}}\mathrm{d}A\right)\mathbf{a} - \int_V \mathbf{F}\mathbf{p}\,\mathrm{d}V - \int_{A_S} \mathbf{F}\mathbf{s}\,\mathrm{d}A = 0 \quad (47)$$

$$\int_V \mathbf{g}\,\mathbf{H}^{\mathrm{T}}\mathrm{d}V\,\dot{\mathbf{w}} = 0 \quad (48)$$

In the standard case, a unique solution exists if a given pressure acts on the top and bottom faces of the solution area. Alternatively, a velocity and a displacement distribution may be given. The absence of a fixed boundary in the vertical direction leads to a kinematical system. For stability, a single node has to be fixed. However, no force is allowed to act on the fixed node at the end of the calculation.

Considering a real silo with a relatively small opening, it is reasonable to assume that the pressure on the opening vanishes in the beginning of the discharging. This leads to a reduction of the average pressure on the bottom face.

7 SINGLE ELEMENT SYSTEM

The feasibility of the model will be demonstrated with a simple example. The standard case is represented by a single element. The height is H, the width is L.

7.1 Solid analysis

7.1.1 Constant strain element

Node 1 is at the top and node 2 is at the bottom of the system.

Displacement function:

$$u_1 = \mathbf{f}^{\mathrm{T}}\mathbf{w} = \begin{pmatrix} \frac{H - x_1}{H} & \frac{x_1}{H} \end{pmatrix} \cdot \begin{pmatrix} w_1 \\ w_2 \end{pmatrix} \quad (49)$$

Equation system without boundary conditions:

$$\left[\frac{L}{H} \cdot \frac{E(1-\nu)}{(1+\nu)(1-2\nu)} \cdot \begin{pmatrix} 1 & -1 \\ -1 & 1 \end{pmatrix} + \frac{\mu\nu E}{(1+\nu)(1-2\nu)} \cdot \begin{pmatrix} 1 & -1 \\ 1 & -1 \end{pmatrix}\right] \cdot \begin{pmatrix} w_1 \\ w_2 \end{pmatrix} = \ldots$$

$$\ldots = \frac{\gamma HL}{2}\begin{pmatrix}1\\1\end{pmatrix} + L\begin{pmatrix}s_1\\s_2\end{pmatrix} \tag{50}$$

s_1 acts on the top face, s_2 acts on the bottom face.

(I) The bottom face is fixed

$$w_2 = 0 \tag{51}$$

$$w_1 = \left(\frac{\gamma H}{2} + s_1\right)\cdot\frac{HL}{E}\cdot\frac{(1+\nu)(1-2\nu)}{(1-\nu)L + H\mu\nu} \tag{52}$$

$$s_2 = -\frac{2L(1-\nu)}{L(1-\nu)+H\mu\nu}\cdot\frac{\gamma H}{2} + \left(1 - \frac{2L(1-\nu)}{L(1-\nu)+H\mu\nu}\right)\cdot s_1 \tag{53}$$

$$\boldsymbol{\sigma} = -\left(\frac{\gamma H}{2} + s_1\right)\cdot\frac{L(1-\nu)}{L(1-\nu)+H\mu\nu}\cdot\begin{pmatrix}1\\ \dfrac{\nu}{(1-\nu)}\\ 0\end{pmatrix} \tag{54}$$

The effect of Coulomb friction is restricted to an increased stiffness. It reduces the top settlement from eq. (56) to eq. (52).

The coefficient of wall friction is set to zero.

$$\mu = 0 \tag{55}$$

$$w_1 = \left(\frac{\gamma H}{2} + s_1\right)\cdot\frac{H}{E}\cdot\frac{(1+\nu)(1-2\nu)}{1-\nu} \tag{56}$$

$$s_2 = -\gamma H - s_1 \tag{57}$$

$$\boldsymbol{\sigma} = -\left(\frac{\gamma H}{2} + s_1\right)\cdot\begin{pmatrix}1\\ \dfrac{\nu}{(1-\nu)}\\ 0\end{pmatrix} \tag{58}$$

(II) Standard case

$$s_2 = -s_1 = -s \tag{59}$$

$$w_1 = w_2 + \frac{\gamma HL}{2}\cdot\frac{(1+\nu)(1-2\nu)}{\mu\nu E} \tag{60}$$

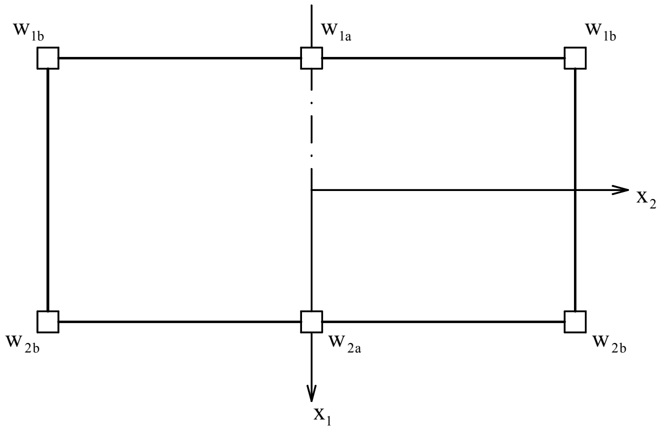

Fig. 3. Nodal displacements

$$s = \frac{\gamma L(1-\nu)}{2\mu\nu} \tag{61}$$

A solution in the standard case is only possible if the top load amounts (61). It results a higher order single element patch test including the natural boundary conditions [8].

7.1.2 Quadratic linear element

Two degrees of freedom w_{1b} on the wall and w_{1a} in the axis represent the displacements of the top face. Analogously, w_{2b} and w_{2a} represent the displacements of the bottom face. Horizontal displacements are excluded. The vertical displacements depend on x_1 and x_2.

$$u_1 = \mathbf{f}^T \mathbf{w} = \frac{1}{HL^2} \cdot \left(\left(L^2 - 4x_2^2\right)\left(H - x_1\right) \quad 4x_2^2\left(H - x_1\right) \quad \left(L^2 - 4x_2^2\right)x_1 \quad 4x_2^2 x_1 \right) \cdot \begin{pmatrix} w_{1a} \\ w_{1b} \\ w_{2a} \\ w_{2b} \end{pmatrix} \tag{62}$$

$$\left[\frac{EL(1-\nu)}{15H(1+\nu)(1-2\nu)} \cdot \begin{pmatrix} 8 & 2 & -8 & -2 \\ 2 & 3 & -2 & -3 \\ -8 & -2 & 8 & 2 \\ -2 & -3 & 2 & 3 \end{pmatrix} + \frac{4}{9} \cdot \frac{E \cdot H}{L(1+\nu)} \cdot \begin{pmatrix} 2 & -2 & 1 & -1 \\ -2 & 2 & -1 & 1 \\ 1 & -1 & 2 & -2 \\ -1 & 1 & -2 & 2 \end{pmatrix} + \dots \right.$$

$$\left. \dots + \frac{\mu E \nu}{(1+\nu)(1-2\nu)} \cdot \begin{pmatrix} 0 & 0 & 0 & 0 \\ 0 & 1 & 0 & -1 \\ 0 & 0 & 0 & 0 \\ 0 & 1 & 0 & -1 \end{pmatrix} \right] \cdot \begin{pmatrix} w_{1a} \\ w_{1b} \\ w_{2a} \\ w_{2b} \end{pmatrix} = \frac{\gamma HL}{6} \cdot \begin{pmatrix} 2 \\ 1 \\ 2 \\ 1 \end{pmatrix} + \frac{L}{3} \cdot \begin{pmatrix} 2s_1 \\ s_1 \\ 2s_2 \\ s_2 \end{pmatrix} \tag{63}$$

(I) The bottom face is fixed

$$w_{2a} = w_{2b} = 0 \tag{64}$$

The third and fourth equations are redundant. The coefficient of wall friction is set to zero.

$$\mu = 0 \tag{65}$$

$$w_{1a} = w_{1b} = \left(\frac{\gamma H}{2} + s_1\right) \cdot \frac{H}{E} \cdot \frac{(1+\nu)(1-2\nu)}{1-\nu} \tag{66}$$

$$s_2 = -\gamma H - s_1 \tag{67}$$

$$\boldsymbol{\sigma} = -\left(\frac{\gamma H}{2} + s_1\right) \cdot \begin{pmatrix} 1 \\ \dfrac{\nu}{(1-\nu)} \\ 0 \end{pmatrix} \tag{68}$$

Equations (66) to (68) are identical to (56) to (58).

(II) Standard case

$$s_2 = -s_1 = -s \tag{69}$$

$$w_{2a} = w_{2b} + \frac{\gamma L^2}{4E} \cdot (1+\nu) \tag{70}$$

$$w_{1a} = w_{2a} + \frac{\gamma H L}{2} \cdot \frac{(1+\nu)(1-2\nu)}{\mu \nu E} \tag{71}$$

$$w_{1b} = w_{2b} + \frac{\gamma H L}{2} \cdot \frac{(1+\nu)(1-2\nu)}{\mu \nu E} \tag{72}$$

$$s = \frac{\gamma L (1-\nu)}{2 \mu \nu} \tag{73}$$

The results agree with (60) and (61). Stability requires a given displacement. The wall node at the bottom face is fixed.

$$w_{2b} = 0 \tag{74}$$

By this the displacements (70) to (72) are unique.

7.2 Liquid analysis

7.2.1 Constant strain rate element

Velocity function:

$$\dot{u}_1 = \mathbf{f}^T \dot{\mathbf{w}} = \frac{1}{H} \cdot \begin{pmatrix} H - x_1 & x_1 \end{pmatrix} \cdot \begin{pmatrix} \dot{w}_1 \\ \dot{w}_2 \end{pmatrix} \tag{75}$$

Pressure function:

$$a = \mathbf{f}^T \mathbf{a} = \frac{1}{H} \cdot \begin{pmatrix} H - x_1 & x_1 \end{pmatrix} \cdot \begin{pmatrix} a_1 \\ a_2 \end{pmatrix} \tag{76}$$

Equation system without boundary conditions:

$$2\eta \frac{L}{H} \cdot \begin{pmatrix} 1 & -1 \\ -1 & 1 \end{pmatrix} \cdot \begin{pmatrix} \dot{w}_1 \\ \dot{w}_2 \end{pmatrix} + \left[\frac{L}{2} \cdot \begin{pmatrix} -1 & -1 \\ 1 & 1 \end{pmatrix} + \frac{\mu H}{3} \cdot \begin{pmatrix} -2 & -1 \\ -1 & -2 \end{pmatrix} \right] \cdot \begin{pmatrix} a_1 \\ a_2 \end{pmatrix} = \ldots$$

$$\ldots = \frac{\gamma HL}{2} \cdot \begin{pmatrix} 1 \\ 1 \end{pmatrix} + L \cdot \begin{pmatrix} s_1 \\ s_2 \end{pmatrix} \tag{77}$$

Continuity condition:

$$\int_V \mathbf{f}\, \mathbf{h}^T dV \dot{\mathbf{w}} = \mathbf{0} \tag{78}$$

$$\frac{L}{2} \cdot \begin{pmatrix} -1 & 1 \\ -1 & 1 \end{pmatrix} \cdot \begin{pmatrix} \dot{w}_1 \\ \dot{w}_2 \end{pmatrix} = \begin{pmatrix} 0 \\ 0 \end{pmatrix} \tag{79}$$

Both equations are equal. Continuity requires the identity of the two nodal velocities.

$$\dot{w}_1 = \dot{w}_2 \tag{80}$$

The velocity term in eq. (77) becomes zero.

Pressure boundary conditions:

$$\begin{aligned} a_1 &= -s_1 \\ a_2 &= s_2 \end{aligned} \tag{81}$$

(I) The coefficient of wall friction is set to zero.

$$\mu = 0 \tag{82}$$

$$s_2 = -\gamma H - s_1 \tag{83}$$

(II) Standard case

$$s_2 = -s_1 = -s \tag{84}$$

$$s = \frac{\gamma L}{2\mu} \tag{85}$$

This again is a higher order single element patch test [8]. The surface loads determine the nodal pressures a_1 and a_2. It remains one velocity degree of freedom and no pressure degree of freedom.

7.2.2 Quadratic linear element

$$\dot{u}_1 = \mathbf{f}^T \dot{\mathbf{w}} = \frac{1}{HL^2} \cdot \left(\left(L^2 - 4x_2^2\right)\left(H - x_1\right) \quad 4x_2^2\left(H - x_1\right) \quad \left(L^2 - 4x_2^2\right)x_1 \quad 4x_2^2 x_1 \right) \cdot \begin{pmatrix} \dot{w}_{1a} \\ \dot{w}_{1b} \\ \dot{w}_{2a} \\ \dot{w}_{2b} \end{pmatrix} \tag{86}$$

$$a = \mathbf{f}^T \mathbf{a} = \frac{1}{H} \cdot \left(H - x_1 \quad x_1 \right) \cdot \begin{pmatrix} a_1 \\ a_2 \end{pmatrix} \tag{87}$$

$$\left[\frac{2}{15} \cdot \eta \cdot \frac{L}{H} \cdot \begin{pmatrix} 8 & 2 & -8 & -2 \\ 2 & 3 & -2 & -3 \\ -8 & -2 & 8 & 2 \\ -2 & -3 & 2 & 3 \end{pmatrix} + \frac{8}{9} \cdot \eta \cdot \frac{H}{L} \cdot \begin{pmatrix} 2 & -2 & 1 & -1 \\ -2 & 2 & -1 & 1 \\ 1 & -1 & 2 & -2 \\ -1 & 1 & -2 & 2 \end{pmatrix} \right] \cdot \begin{pmatrix} \dot{w}_{1a} \\ \dot{w}_{1b} \\ \dot{w}_{2a} \\ \dot{w}_{2b} \end{pmatrix} + \ldots$$

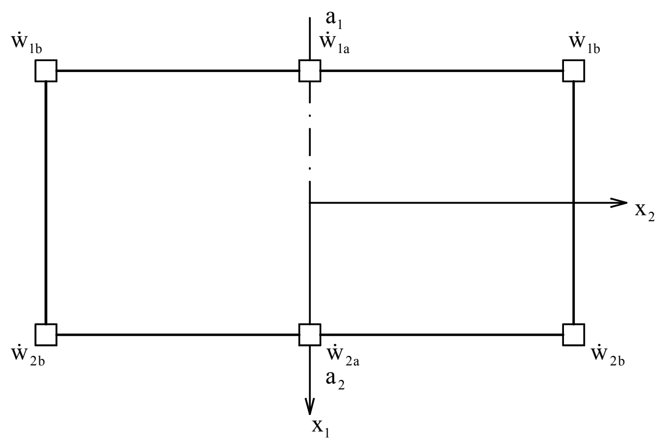

Fig. 4. Nodal velocities and pressures

$$\ldots + \left[\frac{L}{6} \cdot \begin{pmatrix} -2 & -2 \\ -1 & -1 \\ 2 & 2 \\ 1 & 1 \end{pmatrix} - \frac{\mu \cdot H}{3} \cdot \begin{pmatrix} 0 & 0 \\ 2 & 1 \\ 0 & 0 \\ 1 & 2 \end{pmatrix} \right] \cdot \begin{pmatrix} a_1 \\ a_2 \end{pmatrix} = \frac{\gamma HL}{6} \cdot \begin{pmatrix} 2 \\ 1 \\ 2 \\ 1 \end{pmatrix} + \frac{L}{3} \cdot \begin{pmatrix} 2s_1 \\ s_1 \\ 2s_2 \\ s_2 \end{pmatrix} \tag{88}$$

Continuity condition:

$$\frac{L}{30}\cdot\begin{pmatrix} -8 & 2 & 8 & -2 \\ 2 & -3 & -2 & 3 \\ -8 & 2 & 8 & -2 \\ 2 & -3 & -2 & 3 \end{pmatrix}\cdot\begin{pmatrix} \dot{w}_{1a} \\ \dot{w}_{1b} \\ \dot{w}_{2a} \\ \dot{w}_{2b} \end{pmatrix} = \mathbf{0} \tag{89}$$

The continuity is satisfied for:

$$\dot{w}_{1a} = \dot{w}_{2a}$$

$$\dot{w}_{1b} = \dot{w}_{2b} \tag{90}$$

This is due to the fact that no horizontal velocity is possible. Eq. (88) is transformed into an equation system of four unknowns.

Pressure boundary conditions:

$$\begin{aligned} a_1 &= -s_1 \\ a_2 &= s_2 \end{aligned} \tag{91}$$

(I) The coefficient of wall friction is set to zero.

$$\mu = 0 \tag{92}$$

$$\dot{w}_{1a} = \dot{w}_{1b} \tag{93}$$

$$s_2 = -\gamma H - s_1 \tag{94}$$

(II) Standard case

$$s_2 = -s_1 = -s \tag{95}$$

$$s = \frac{\gamma L}{2\mu} \tag{96}$$

$$\dot{w}_{1a} = \dot{w}_{1b} + \frac{\gamma L^2}{8\eta} \tag{97}$$

Again the surface loads determine the nodal pressures completely. One nodal velocity is prescribed for stability, e. g. $\dot{w}_{1b} = 0$, the other three nodal velocities are free.

7.3 Hybrid solid-liquid model

7.3.1 Constant strain/constant strain rate element

The investigation starts with eqs. (47) and (48). All matrices have been derived in chapters 7.1.1 and 7.2.1. Eq. (50) governs the solid solution. Eq. (77) governs the liquid solution.

$$\left[\frac{L}{H}\cdot\frac{E(1-\nu)}{(1+\nu)(1-2\nu)}\cdot\begin{pmatrix}1 & -1\\ -1 & 1\end{pmatrix}+\frac{\mu\nu E}{(1+\nu)(1-2\nu)}\cdot\begin{pmatrix}1 & -1\\ 1 & -1\end{pmatrix}\right]\cdot\begin{pmatrix}w_1\\ w_2\end{pmatrix}+\ldots$$

$$\ldots+2\eta\frac{L}{H}\cdot\begin{pmatrix}1 & -1\\ -1 & 1\end{pmatrix}\cdot\begin{pmatrix}\dot{w}_1\\ \dot{w}_2\end{pmatrix}+\left[\frac{L}{2}\cdot\begin{pmatrix}-1 & -1\\ 1 & 1\end{pmatrix}+\frac{\mu H}{3}\cdot\begin{pmatrix}-2 & -1\\ -1 & -2\end{pmatrix}\right]\cdot\begin{pmatrix}a_1\\ a_2\end{pmatrix}=\ldots$$

$$\ldots=\frac{\gamma HL}{2}\cdot\begin{pmatrix}1\\ 1\end{pmatrix}+L\cdot\begin{pmatrix}s_1\\ s_2\end{pmatrix} \tag{98}$$

The continuity condition for the liquid part results in:

$$\dot{w}_1=\dot{w}_2 \tag{99}$$

Boundary condition for the solid part:

$$w_2=0 \tag{100}$$

(I) System without top loading

$$\begin{aligned}s_1&=0\\ a_1&=0\end{aligned} \tag{101}$$

$$w_1=\frac{H}{6E}\cdot\frac{(3L+2\mu H)(1+\nu)(1-2\nu)}{1-\nu+H\mu\nu-2\nu E(3L+2\mu H)}\cdot\left[\frac{3\gamma H}{3L+2\mu H}-\frac{\gamma}{\mu}-\frac{1}{\mu H}\cdot s_2\right] \tag{102}$$

$$a_2=\frac{\nu}{3}\cdot\frac{3L+2\mu H}{1-\nu+H\mu\nu-2\nu E(3L+2\mu H)}\cdot\left[\frac{3\gamma H}{3L+2\mu H}-\frac{\gamma}{\mu}-\frac{1}{\mu H}\cdot s_2\right]-\frac{\gamma L}{\mu}-\frac{L}{\mu H}\cdot s_2 \tag{103}$$

The coefficient of wall friction is set to zero.

$$\mu=0 \tag{104}$$

$$w_1=(\gamma H+a_2)\cdot\frac{H}{2}\cdot\frac{(1+\nu)(1-2\nu)}{E(1-\nu)} \tag{105}$$

$$s_2=-\gamma H \tag{106}$$

The mere solid solution (56) requires the additional condition a_2 = 0. For absent wall friction a unique solution is not possible.

(II) Standard case

$$\begin{aligned}a_2&=a_1=a\\ s_2&=-s_1=-s\end{aligned} \tag{107}$$

$$w_1 = \frac{H}{E} \cdot (1+\nu) \cdot \left(s - \frac{\gamma L}{2\mu} \right) \tag{108}$$

$$a = \frac{\nu}{1-2\nu} \cdot s - \frac{\gamma L}{2\mu} \cdot \frac{1-\nu}{1-2\nu} \tag{109}$$

(i) Mere solid behavior:

Eq. (61) represents the surface load of mere solid behavior.

$$s = \frac{\gamma L (1-\nu)}{2\mu\nu} \tag{110}$$

It follows:

$$w_1 = \frac{\gamma H L}{2} \cdot \frac{(1+\nu)(1-2\nu)}{\mu \nu E} \tag{111}$$

$$a = 0 \tag{112}$$

Eq. (111) agrees with the solution of the solid model (60).

(ii) Mere liquid behavior:

Eq. (85) represents the surface load of mere liquid behavior.

$$s = -s_2 = \frac{\gamma L}{2\mu} \tag{113}$$

It follows:

$$w_1 = 0 \tag{114}$$

$$a = -s \tag{115}$$

Eq. (115) agrees with the pressure boundary conditions (81).

Mere solid and mere liquid behavior result from the limiting surface loads s. It is reasonable to assume that between these two limiting loads the hybrid model will lead to an unique solution.

The following discussion deals with pressures that exceed the two limiting values and result either in extensive compression ore in the loss of continuity.

If the surface loads decrease beyond the admissible level, negative displacements result. The compression of the liquid component increases. The extended solid part prestresses the liquid part.

If the surface loads exceed the admissible level the vertical top displacement increases. The liquid pressure enters the tension range. By this the resulting wall pressure continues to hold the equilibrium to the weight of the filling. It is directed upward extensively by the solid part and redirected by the downward component of the liquid part.

7.3.2 Quadratic linear element

$$\left[\frac{EL(1-\nu)}{15H(1+\nu)(1-2\nu)}\cdot\begin{pmatrix}8 & 2 & -8 & -2\\ 2 & 3 & -2 & -3\\ -8 & -2 & 8 & 2\\ -2 & -3 & 2 & 3\end{pmatrix}+\frac{4}{9}\cdot\frac{E\cdot H}{L(1+\nu)}\cdot\begin{pmatrix}2 & -2 & 1 & -1\\ -2 & 2 & -1 & 1\\ 1 & -1 & 2 & -2\\ -1 & 1 & -2 & 2\end{pmatrix}+\dots\right.$$

$$\left.\dots+\frac{\mu E\nu}{(1+\nu)(1-2\nu)}\cdot\begin{pmatrix}0 & 0 & 0 & 0\\ 0 & 1 & 0 & -1\\ 0 & 0 & 0 & 0\\ 0 & 1 & 0 & -1\end{pmatrix}\right]\cdot\begin{pmatrix}w_{1a}\\ w_{1b}\\ w_{2a}\\ w_{2b}\end{pmatrix}+\dots$$

$$\dots+\left[\frac{2}{15}\cdot\eta\cdot\frac{L}{H}\cdot\begin{pmatrix}8 & 2 & -8 & -2\\ 2 & 3 & -2 & -3\\ -8 & -2 & 8 & 2\\ -2 & -3 & 2 & 3\end{pmatrix}+\frac{8}{9}\cdot\eta\cdot\frac{H}{L}\cdot\begin{pmatrix}2 & -2 & 1 & -1\\ -2 & 2 & -1 & 1\\ 1 & -1 & 2 & -2\\ -1 & 1 & -2 & 2\end{pmatrix}\right]\cdot\begin{pmatrix}\dot{w}_{1a}\\ \dot{w}_{1b}\\ \dot{w}_{2a}\\ \dot{w}_{2b}\end{pmatrix}+\dots$$

$$\dots+\left[\frac{L}{6}\cdot\begin{pmatrix}-2 & -2\\ -1 & -1\\ 2 & 2\\ 1 & 1\end{pmatrix}-\frac{\mu\cdot H}{3}\cdot\begin{pmatrix}0 & 0\\ 2 & 1\\ 0 & 0\\ 1 & 2\end{pmatrix}\right]\cdot\begin{pmatrix}a_1\\ a_2\end{pmatrix}=\frac{\gamma HL}{6}\cdot\begin{pmatrix}2\\ 1\\ 2\\ 1\end{pmatrix}+\frac{L}{3}\cdot\begin{pmatrix}2s_1\\ s_1\\ 2s_2\\ s_2\end{pmatrix} \qquad (116)$$

The continuity condition for the liquid part results in:

$$\dot{w}_{1a}=\dot{w}_{2a}$$

$$\dot{w}_{1b}=\dot{w}_{2b} \qquad (117)$$

Boundary condition for the solid part:

$$w_{2b}=0 \qquad (118)$$

Boundary condition for the liquid part:

$$\dot{w}_{2b}=0 \qquad (119)$$

(I) System without top loading

$$s_1=0$$

$$a_1=0 \qquad (120)$$

The bottom face is fixed for the solid part:

$$w_{2a}=0 \qquad (121)$$

The remaining four unknowns are the displacements w_{1a} and w_{1b} on the top face, the velocity $\dot{w}_{1a}$ in the centre of the bottom face and the pressure a_2 on the bottom face. They depend on the bottom load s_2.

8 CONCLUSION

Granular material is a very complex matter. It has solid as well as liquid properties and is supposed to have no tensile strength. If it is subjected to steady state flow in an infinite high tube (standard case) its behavior becomes transparent. The formulation of appropriate constitutive equations leads to a hybrid solid-liquid description. Single element systems show the feasibility of the presented model.

REFERENCES

[1] K.-J. Bathe, *Finite-Elemente-Methoden*. Springer Verlag, Berlin, 2002.

[2] L. S. Das and J. T. Jenkins, Collisional Flows of Identical, Smooth, Nearly Elastic Spheres in a Vertical Chute. R. Garcia-Rojo, H. J. Herrmann and S. McNamara eds. *Powders and Grains*, Stuttgart, 2005.

[3] M. Göttlicher, Flow of Granular Material in Tall Silos. Z. H. Yao, M. W. Yuan, W. X. Zhong eds. *Proceedings of the Sixth World Congress on Computational Mechanics*, Beijing, 2004.

[4] R. M. Nedderman and C. Laohakul, The Thickness of the Shear Zone of Flowing Granular Materials, *Powder Technology*, **25**, 91-100, 1980.

[5] O. Pouliquen, C. Cassar, Y. Forterre, P. Jop and M. Nicolas, How Do Grains Flow, Towards a Simple Rheology for Dense Granular Flows. R. Garcia-Rojo, H. J. Herrmann and S. McNamara eds. *Powders and Grains*, Stuttgart, 2005.

[6] O. Pouliquen and R. Gutfraind, Stress Fluctuations and Shear Zones in Quasi-Static Granular Flows. *Phys. Rev.,* **53**, 552-561, 1996.

[7] S. B. Savage, Gravity Flow of Cohesionless Granular Materials in Chutes and Channels. *Journal of Fluid Mechanics*, **92**, 53-96, 1979.

[8] Zienkiewicz, O. C. and Taylor, R. L., *The Finite Element Method, Vol. 1, The Basis, 5th edn*. Prentice-Hall Inc., Butterworth-Heinemann, Oxford, 2000.

[9] Zienkiewicz, O. C. and Taylor, R. L., *The Finite Element Method, Vol. 3, Fluid Dynamics, 5th edn*. Butterworth-Heinemann, Oxford, 2000.